Integration of second-life batteries in residential microgrids and fast charging stations

Idoia San Martín, Elisa Braco, Álvaro Martín, Pablo Sanchis, Alfredo Ursúa
Department of Electrical, Electronic and Communication Engineering
Institute of Smart Cities. Public University of Navarre
Campus Arrosadia, 31006, Pamplona, Spain
idoia.sanmartin@unavarra.es, elisa.braco@unavarra.es, alvaro.martin@unavarra.es, pablo.sanchis@unavarra.es, alfredo.ursua@unavarra.es

***Abstract*—The potential of batteries from electric vehicles to be given a second life in stationary applications could be starting to become a reality in few years. However, the technical and economic feasibility of such second-life batteries (SLBs) is still uncertain. In this context, this paper analyses the real operation of a SLB in three scenarios: two of residential microgrids with photovoltaic generation under different strategies, and a fast charging station for electric mobility. To this end, three energy management strategies are developed, the first of which seeks to maximise the self-consumption of a typical household with photovoltaic generation; the second, in addition to maximising self-consumption, presents a night-time charge and peak shaving of the contract power from the grid; and the last refers to an urban bus charging station in which the aim is to reduce the contract power from the grid. Experimental validation of SLB during more than three weeks of operation in each of the scenarios have proved the technical viability of these batteries in the applications analysed.**

Keywords—Second-Life batteries, Li-ion batteries, Electric vehicles, residential microgrids, fast charging stations.

I. INTRODUCTION

The number of electric vehicles (EVs) on our roads is growing at a spectacular rate. In 2021 6.6 million EVs were sold, more than twice that of the previous year, resulting in 16 million EVs on our roads according to IEA data [1]. In the coming years, this upward trend is expected to continue, with more than 140 million EVs on the road by 2030. This expansion has direct consequences on the demand for lithium-ion batteries for EVs.

Due to usage and time lapse, lithium-ion batteries lose power and energy capabilities, in such a way that their operation in EVs is even compromised. Therefore, automotive regulations set as withdrawal point from EVs when their capacity reaches 70-80 % of its initial value. In recent years, the reuse of these batteries as storage systems in stationary applications, with operating profiles less demanding than EVs, and lower energy and power density requirements, has emerged as an alternative to direct recycling.

There are currently many uncertainties regarding the economic feasibility of reusing EV batteries. On the one hand, the cost of these second-life batteries (SLBs) should be lower than the new ones. Their main disadvantages compared to new batteries are related to their lower energy and power capabilities and their heterogeneity. These issues may be overcome with adequate battery sizing, cell grouping and specific controls implemented in the Battery Management System (BMS) [2, 3].

We would like to acknowledge the support of the Spanish State Research Agency (AEI) grant PID2019-111262RB-I00/AEI/10.13039/501100011033, the European Union H2020 Project STARDUST (74094). E. Braco was supported by a Predoctoral Contract of the Government of Navarra.

SLBs are good candidates for different stationary applications: grid-connected, off-grid or electric mobility-related systems [4-6]. Regarding grid-connected installations, SLBs are able to provide grid services such as peak shaving [7] or frequency regulation [8]; as well as be part of microgrids, smart grids or self-consumption systems [9-12]. In relation to off-grid systems, SLBs aim to ensure electricity supply in the absence of, for example, wind and/or photovoltaic resources [13]. Moreover, they could be used in applications related to electric mobility, such as charging stations, thus reducing grid-contracted power [14, 15]. The integration of reused batteries in these systems supports the technical feasibility, thereby contributing to SL market success.

This work focuses on the integration of a SLB in three different real-life scenarios. To this end, a repurposed battery with modules from Nissan Leaf EVs is tested in a real microgrid, under three energy strategies. The first strategy is based on maximising the self-consumption of a residential household with photovoltaic (PV) generation; the second, in addition to maximising self-consumption, considers night-time charging and peak shaving; and the last recreates a fast charging station for a city bus in which the aim is to reduce the power contracted by the grid.

The paper is structured in 5 sections. Section II details the experimental setup, including a description of the SLB and the experimental microgrid where the tests are carried out. Section III describes the energy management strategies developed and Section IV presents the experimental validation of the strategies and a comparison among them. Finally, the conclusions are presented in Section V.

II. EXPERIMENTAL SETUP

A. Second-life battery description

The tested SLB is a prototype battery, which has nominal specifications for energy, power and voltage 4 kWh, 4 kW and 90 V respectively. It consists of 12 modules as shown in Fig. 1 connected in series. Each module is formed by 4 pouch cells with graphite anode and LMO/LNO cathode, connected in 2s2p configuration.

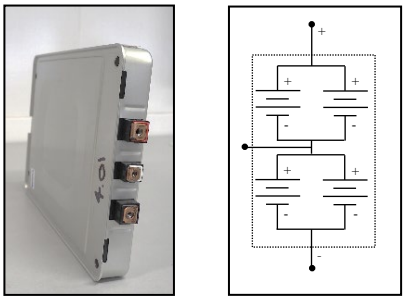

Fig. 1. Nissan Leaf module and internal schematic.

B. Experimental microgrid

The tests are carried out in the microgrid of the Public University of Navarre (UPNA), shown in Fig. 2. The microgrid has a mixed AC architecture, which includes a real 4.5 kWp PV installation, a PV inverter (INGECON SUN 1Play 6TL of 6 kW from Ingeteam Power Technology) and two inverters to connect the batteries (INGECON SUN STORAGE 1Play 6 TL of 6 kW, also from Ingeteam Power Technology). It also comprises a control unit that manages the system and allows implementing different energy management strategies, as well as monitoring and measuring system for voltages, currents and power.

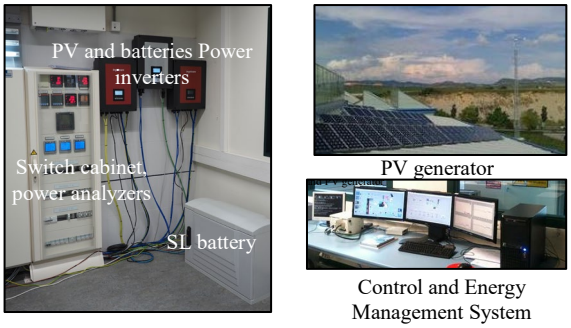

Fig. 2. Experimental microgrid located at the Public University of Navarre.

C. Full characterization test

In order to assess the state of the SLB before and after implementing the strategies, a complete full characterization test is carried out, which consists of:

- Capacity and energy test: sequence of 3 full cycles at $C/3$ with constant current between the maximum and minimum state of charge (SOC). Battery capacity and energy are defined according to the discharge values of the third cycle. C is determined according to the nominal capacity of the battery.
- Efficiency test: sequence of 3 full cycles at maximum constant power in charge and discharge between the maximum and minimum SOC. Between each cycle, 1 hour of rest is left to stabilize voltage. Energy efficiency is defined from the data of the third cycle.
- Internal resistance test: sequence of discharge and charge pulses with constant power at $P_n/2$ at specific SOC levels with 1-hour rest between pulses. The SOC levels are: SOC maximum, 90 %, 70 %, 70 %, 50 %, 30 %, 15 % and SOC minimum. Resistance is measured between the 10-second pulse and rest.

Fig. 3 shows the complete characterisation test with the evolution of SOC, battery voltage (V_b) and battery current (I_b). The characterisation tests are performed in the battery operating range determined between SOC 10 and 97 %.

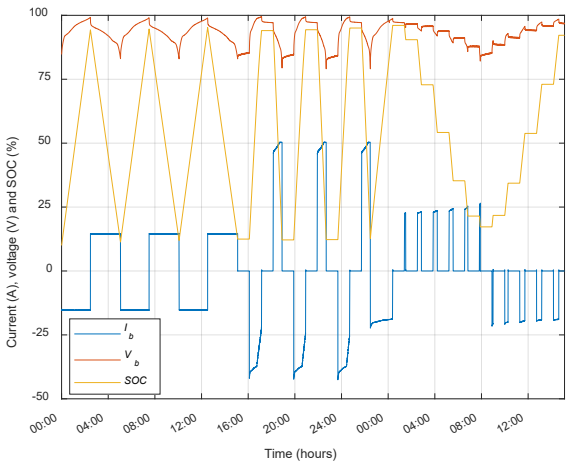

Fig. 3. Current (I_b), voltage (V_b) and State of Charge (SOC) measured in a full characterization test.

III. Description of the Energy Management Strategies

In order to analyse the behaviour of the SLB, three energy strategies are developed. Strategies 1 and 2 are based on maximising self-consumption, but strategy 2 also adds night-time charging and reduces the peak power consumed from the grid. Finally, strategy 3 targets a fast charging station for a city bus. These strategies are programmed in the microgrid control and management system and experimentally tested for several weeks.

A. Strategy 1: maximising self-consumption in a residential household

Strategy 1 considers a grid-connected house with PV panels in which an SLB is integrated, as shown in Fig. 4. This system is composed of two inverters (PV and battery) with a common AC bus connected to the grid and to the loads.

The main objective of strategy 1 is maximising the self-consumption of the residential household. The scheme of this strategy is shown in Fig. 4. As can be seen, to maximise self-consumption, the net power (P_{net}) is obtained from the PV power generated (P_{PV}) and the loads consumption (P_c):

$$P_{net} = P_{PV} - P_c \quad (1)$$

In case P_{net} is positive and the SOC is lower than the maximum, the SLB is charged ($P_b = P_{net}$). P_b is limited to the nominal value, and if surpassed ($P_b < P_{b,max}$), the surplus is fed into the grid. In case the battery is already charged ($SOC = SOC_{max}$), the remaining power is supplied to the grid ($P_g = P_{net}$). On the other hand, if power demand is greater than generation, i.e. $P_{net} < 0$, priority is given to discharging the battery to supply the consumption ($P_b = P_{net}$). In case the battery is completely discharged ($SOC = SOC_{min}$), the grid responds to consumption ($P_g = P_{net}$).

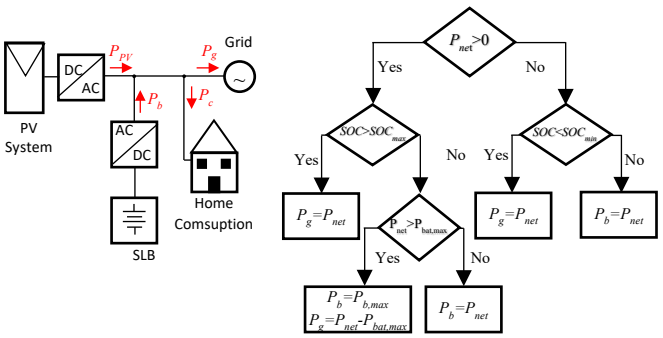

Fig. 4. Schematic of residential microgrid and strategy 1: maximising self-consumption in a residential household.

B. *Strategy 2: maximum self-consumption, night cycle and peak shaving in residential household*

Strategy 2 is applied to the same system as strategy 1, and in addition to maximising self-consumption, it includes night charging and consumption peak shaving. The objective of night charging is to benefit from lower costs of energy, motivated for example by the wind power excess, to charge the battery, thereby responding to the consumption at the beginning of the day when the cost of electricity is higher. On the other hand, the objective of peak shaving is to limit the contracted power of the grid. To do this, a peak shaving value (P_{ps}) is defined, lower than the current installed power. In order for the battery to be able to provide these consumption peaks, a part of the battery's energy is reserved, which is limited by SOC_{ps}.

The schematic of strategy 2 is shown in Fig. 5. In case the generated power is higher than the consumed power, i.e. P_{net} is positive, and the SLB is charged to the maximum ($SOC = SOC_{max}$). P_{net} is supplied to the grid ($P_g = P_{net}$). Conversely, if the SLB does not reach the maximum charge, the SLB is charged, i.e. $P_b = P_{net}$ as long as P_{net} is lower than the maximum power of the SLB. In case it is higher, the SLB is charged to its maximum power ($P_b = P_{b,max}$) and the surplus is fed into the grid ($P_g = P_{net}$-$P_{b,max}$). In the opposite case, when consumption is greater than generation ($P_{net} < 0$), two situations may arisewe. If the SOC is greater than the SOC_{ps}, the SLB covers the consumption ($P_b = P_c$) up to its maximum power, and with the rest covered by the grid. The other situation occurs when the SOC is lower than the SOC_{ps}. In this case, when P_c is higher than P_{ps}, the grid power is limited to the peak shaving value, i.e. $P_g = P_{ps}$ and the rest is covered by the SLB ($P_b = P_c$-P_{ps}), while when P_c is lower than P_{ps}, the grid covers the consumption, $P_g = P_c$.

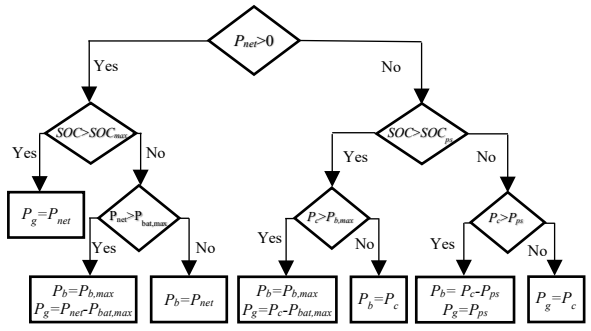

Fig. 5. Schematic of strategy 2: maximum consumption, night cycle and peak shaving in residential household.

C. *Strategy 3: fast charging station for electrical mobility*

Strategy 3 focuses on fast charging of city buses. Fig. 6 shows the schematic of the charging station consisting of two inverters with a common AC bus connected to the grid, one of the inverters being for the SLB and the other for the load. A schematic of strategy 3 is also shown in the figure. The objective of the SLB is to reduce the contracted grid power at the charging station. For this purpose, the power to be supplied by the battery (P_b) is the difference between the maximum grid power ($P_g = P_{g,max}$) and the power required for bus charging (P_{bus}). The battery charging process occurs when there is no bus, with a power depending on the time available until the next bus arrives, which is known in advance based on the position information sent by the buses. If there is no time to fully charge the battery, the SLB charge is set to the maximum power, i.e. $P_b = P_{g,max}$, whereby this power is equal to or less than the maximum battery charging power.

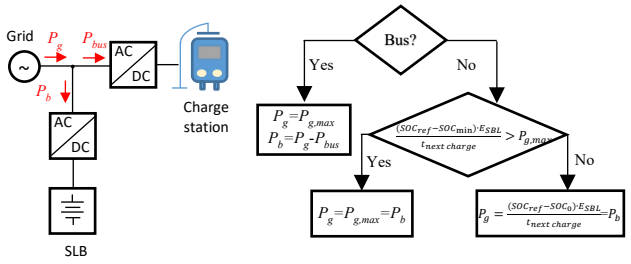

Fig. 6. Schematic of fast charging station and strategy 3: fast charging station for electrical mobility.

IV. Results and Discusion

A. *Experimental validation of strategy 1: maximising self-consumption in a residential household*

As mentioned above, strategy 1 is applied to a grid-connected house with PV generation. It is based on the annual data of PV power measured in real time of the installation located on the roof of the Los Pinos Building of the UPNA and the consumption profile corresponding to a real single-family house located in the Pamplona region, which is emulated in the microgrid. Before programming the strategy in the microgrid, the generation and consumption data are sized and scaled according to the tested SLB. Specifically, with the annual generation and consumption data, the daily energy consumed (E_{con}) and generated (E_{PV}) are calculated. These values are then scaled with the assumption that the total energy of the SLB is 20 % of E_{con} and the E_{PV} is 90 % of E_{con}, considered as typical values for residential self-consumption installations [16]. As a result, the daily average energy consumption of the house is 20.2 kWh and the daily average PV energy generated is 18 kWh. The strategy is experimentally tested during 31 days, namely from 11th August to 9th September 2020.

Fig. 7 shows the P_{PV}, P_b, P_c, P_g and SOC measured during one week of operation of the SLB in the system described in subsection III.A and under strategy 1. It can be observed that the SLB performs a complete cycle of charging and discharging per day, starting unloaded ($SOC = SOC_{min} = 10$ %) and being charged when there is excess of PV generation (P_{PV}), until $SOC_{max} = 97$ %. When the SLB is charging, P_b is positive, while P_b is negative when it is discharging. When no PV generation is available ($P_{PV} = 0$), the SLB covers the consumption until it reaches the minimum SOC. In terms of PV generation, there are clearer days, such as day 2, and days

with significant variations caused by the presence of clouds and clearings, such as day 5. With respect to P_c, significant power variations can be seen due to different loads connected throughout the day, such as glass-ceramic hobs or irrigation systems. Night consumption is almost constant and mainly due to the refrigerator and the stand-by mode of different electrical devices. Daytime consumption increases at breakfast (8:00 h), lunch (13:30 h) and dinner (20:00 h) times, consequence of the switching on of electrical devices in the kitchen. In relation to P_g, it is observed that it covers consumption when there is null or not enough PV generation, and if the *SOC* of the SLB is outside the established limits, i.e. *SOC* greater than 97 % or less than 10 % ($P_g < 0$). On the other hand, when there is excess P_{PV} ($P_{PV} > P_c$) it is supplied into the grid ($P_g > 0$).

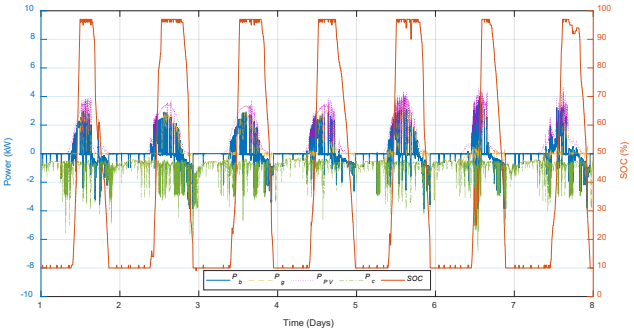

Fig. 7. Evolution of the SLB power (P_b), grid power (P_g) load power (P_c) and PV generation power (P_{PV}) and SOC of the SLB during one week of testing with strategy 1.

B. *Experimental validation of strategy 2: maximum self-consumption, night cycle and peak shaving in residential household*

For the experimental validation of strategy 2, the same PV and load data detailed in the previous subsection is used, although with different sizing. In this case, the total energy of the SLB is 40 % of E_{con} and the E_{PV} is 130 % of E_{con}. This corresponds to a daily average energy consumption of 10 kWh in the household and a daily average PV generation of 14.8 kWh. In this case, the consumption and PV generation data correspond to the period between 1st April 2021 and 30th April 2021. In addition, the P_g is limited to a value of P_{ps}, set at 4 kW and the SOC_{ps} is fixed at 20 %. The strategy is in operation for 29 days in the microgrid of the UPNA described in subsection II.B.

The behaviour of the SLB under strategy 2 is shown in Fig. 8, with the measured P_b, P_g, P_{PV}, P_c and *SOC* during one week. It can be observed that the SLB performs almost two cycles per day, with the diurnal cycle and the nocturnal charge. It is also observed that the P_g does not exceed the 4 kW set for the peak shaving. In the diurnal cycle, the SLB starts charged and is discharged to cover the initial consumption, until the PV generation starts. This PV power is splitted to respond demand and charge the SLB. Once the SLB is charged, the P_{PV} covers the consumption and the remainder is fed into the grid. In turn, the SLB performs peak shaving, preventing P_g from exceeding 4 kW. For example, on day 16 at 13:45h there is consumption load peak of 5.3 kW, ($P_c > P_{ps}$), with the SLB providing 1.3 kW, i.e. the difference between P_c and P_{ps}. At this point, $P_{PV} = 1.5$ kW and $P_g = 2.5$ kW, thus complying with the peak shaving premise. The night cycle begins with the discharge of the battery to cover consumption when there is no more PV generation, i.e., approximately at 19:00 h. If the SLB reaches a *SOC* of 20 %, it is no longer used and the consumption is supplied by the grid. In this way, 20 % of the energy of the SLB is reserved for peak shaving if necessary, i.e. when $P_c > P_{ps}$. In addition, at 00:00 h the SLB charge is programmed, benefiting from the lower electricity price. This charge is carried out until 05:00 h, with low charge power to avoid excessive degradation of the SLB. More precisely, the charge power is. $P_n/6$ which is equivalent to 0.67 kW. In this way, the SLB is fully charged to assume the consumption at the beginning of the day.

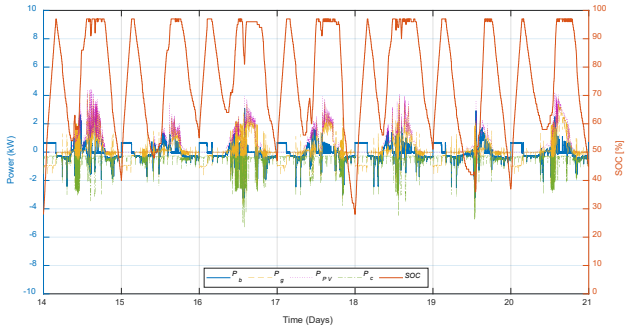

Fig. 8. Evolution of the SLB power (P_b), grid power (P_g) consumption power (P_c) and PV generation power (P_{PV}) and the SLB state of charge (*SOC*) during one week of testing with strategy 2.

C. *Experimental validation of strategy 3: fast charging station for electrical mobility*

To validate strategy 3, real data from a fast charging station of a city bus is used [17]. The charging station receives a bus every 12 minutes, 4 times per hour during a workday, from 07:00 h to 22:30 h. It does not operate on Sundays and holidays. This data is scaled for the SLB under test. More precisely, a P_{bus} of 8 kW, and a P_g of 4 kW are considered. In addition, the allowed operating *SOC* is from 10 % to 97 %. The strategy is programmed in the UPNA microgrid and is implemented for 20 days, more precisely from the 3th to the 24th September 2021.

Fig. 9 shows the P_b, P_g, P_{bus} and the *SOC* of the SLB under test during six days, namely from Monday to Saturday, since this is when the buses circulate. It can be seen that both the SLB and the grid cover the bus charging power, and that P_g is always guaranteed not to exceed the maximum of 4 kW. In relation of the SLB operation, several cycles are observed during the day, corresponding to the charging of the buses. In particular, more than 50 partial cycles (charging and discharging) per day are observed, most of them with a depth of discharge (*DOD*) lower than 20 %, except on day 12, when the SLB reaches a *SOC* of 40 %. This is due to the fact that when the first bus arrives, the initial *SOC* is 76 %. At the beginning of the rest of the days (13 - 17), as the initial *SOC* is higher (approximately 90 %), the SLB is discharging more during the arrival of the first buses, reaching SOC_{max} after the first few cycles. From this moment, the *DOD* is lower than 20 %.

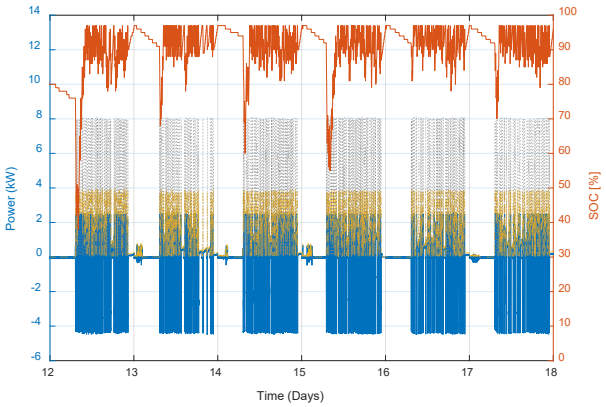

Fig. 9. Evolution of the SLB power (P_b), grid power (P_g) and bus power (P_{bus}) and the SLB state of chage (SOC) during six days of testing with strategy 3.

D. Comparation and discussion

This section aims to analyse and compare the behaviour of the SLB in each scenario. To do so, the results obtained in the complete characterisation of the SLB are firstly analysed in terms of capacity, resistance, energy and energy efficiency before and after each strategy. In a second stage, the behaviour of the SLB in each of the strategies is studied according to the energy throughput in the SLB, the number of full equivalent cycles (FEC), the number of cycles as a function of DOD and the percentage of self-consumption.

Table I shows the results obtained in the full characterisation test described in subsection II.C. Specifically, it shows the capacity, resistance at 50 % of SOC, energy and energy efficiency at the start and end of each of the strategies. It is observed that the capacity decreases by 1.3, 2.2 and 5 Ah after performing under strategies 1, 2 and 3 respectively, while the resistance increases by 1, 3.8 and 1.8 mΩ. In relation to energy, a similar trend to capacity is observed, decreasing by 110, 190 and 460 Wh in strategies 1, 2 and 3 respectively. With regard to energy efficiency, the values obtained at the beginning and at the end of each strategy are similar, ranging between 92.5 and 92.8 %. These efficiencies have been obtained at maximum power in both charging and discharging, and higher values are measured with lower power and/or current. For example at a current of C/3, values between 96.2 and 97.3 % are obtained.

Since the SLB performs during different number of days under each of the strategies, and considering that it is in the linear ageing zone [9], i.e. it has not yet reached the ageing knee, the daily capacity loss and daily resistance increase are calculated. The precise values are 41.9, 75.9 and 250 mAh/day and 0.032, 0.131 and 0.09 mΩ/day in strategies 1, 2 and 3 respectively. Therefore, in the three strategies a reduction in the state of health of the SLB exists. In relation to capacity, the decrease is most notable in strategy 3, reaching a reduction 6 times greater than in strategy 1 and 3.2 times greater than in strategy 2. Analysing the increase in resistance, it is also observed that it is 2.8 times greater in strategy 3 compared to strategy 1, however, in strategy 2 the increase is higher than in strategy 3. The values obtained for resistance may be affected due to the sensitivity of this measure to the test conditions.

TABLE I. RESULTS OF FULL CHARACTERIZATION TEST AT THE BEGINNING (INITIAL) AND AT THE END (FINAL) OF EACH STRATEGY

Strategy		***Capacity (Ah)***	***Resistance (mΩ)***	***Energy (kWh)***	***Efficiency (%)***
Strategy 1	Initial	37.5	48.4	3.44	92.8
	Final	36.2	49.4	3.33	92.5
Strategy 2	Initial	37.3	46.8	3.45	92.7
	Final	35.1	50.6	3.26	92.8
Strategy 3	Initial	35.1	50.6	3.26	92.8
	Final	30.1	52.4	2.80	92.5

On the other hand, an analysis of the SLB behaviour under each strategy is carried out. In relation to the energy throughput, of the SLB in strategy 1, 2 and 3, it is 252.6, 268.2 and 616.2 kWh respectively. That is to say, the energy throughput in strategy 3 is 243.9 % and 229.7 % greater than in strategy 1 and 2. Consequently, the SLB is subject to a higher energy requirement in strategy 3.

Furthermore, the EFC is defined by the ratio of the energy throughput in the SLB (E_b) and its nominal energy (E_n = 4 kWh) by means of Eq. (2):

$$EFC = E_b/(2 \cdot E_n) \tag{2}$$

The EFC is 31.6, 33.5 and 77.0 in strategies 1, 2 and 3 respectively. That is, in strategy 3 the EFC are more than twice the other strategies despite the fact that it lasts 11 and 9 days less than strategies 1 and 2 respectively. In theory, since in strategy 3 the SLB performs more EFC, it will degrade at a higher rate. However, to analyse SLB operation in detail, it is necessary to know at what DOD and current these cycles occur, as these are very influential variables in battery degradation. To obtain the number of cycles as a function of DOD, the rainflow algorithm is applied to the SOC [18]. Fig. 10 shows the number of cycles as a function of DOD for strategy 1, 2 and 3. It is observed that strategy 1 performs most of its cycles, namely 25, at a DOD between 80 and 90 %, while, strategy 3 performs 49 cycles at a DOD between 0 and 10 %. However, in strategy 2, the majority of the cycles, namely 26, are between 40 and 80 % DOD. Not only does the SLB perform more cycles in strategy 3, but also it operates at a higher current, which contributes to a higher degradation, as shown in Table I. With regard to the operation in strategy 1, it is observed that the SLB performs a similar number of cycles but at a higher DOD than in strategy 2. In spite of this, the SLB degrades more during operation under strategy 2, and this may be due to the distribution of the cycles according to the DOD or to aspects related to the BMS such as cell balancing or SOC estimation. These aspects are of crucial importance in BMSs, as the batteries are configured with SL modules that can have a considerable dispersion in both capacity and resistance [3].

On the other hand, an important parameter in grid-connected microgrids is the percentage or degree of self-consumption (G_{sc}), defined in this case as one minus the ratio of energy consumed from the grid ($E_{g,c}$) and the load energy (E_{con}), as shown in Eq. 3.

$$G_{sc} = 1 - E_{g,c}/E_{con} \tag{3}$$

The G_{sc} is calculated for strategies 1 and 2, resulting in and 59.8 % and 58.9 % in strategies 1 and 2 respectively. Therefore, in both cases the dependence on the electrical grid is considerably reduced.

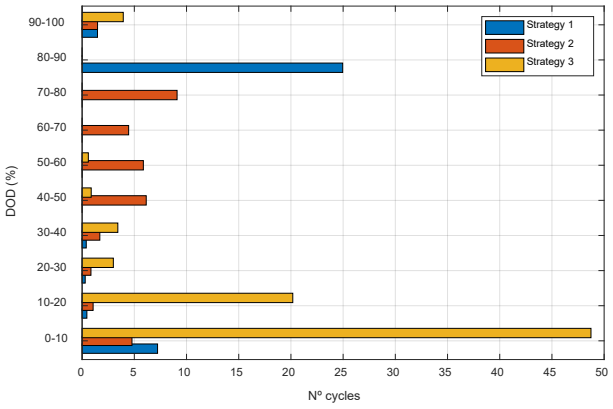

Fig. 10. Number of cycles as a function of depth of discharge (*DOD*) for strategies 1, 2 and 3.

V. CONCLUSION

This article assesses the experimental testing of a SLB in three operating scenarios, two of them related to residential microgrids and another one to a fast charging station for electric mobility. The first one (strategy 1) is based on maximising the self-consumption of a single-family house with photovoltaic generation. The second (strategy 2), in addition to maximising self-consumption in the household, adds a night charge in order to both take advantage of the lower cost of electricity and to have energy available to cover consumption at the beginning of the day, when photovoltaic generation is minimal. This strategy also includes peak shaving to reduce the contracted power from the grid and reduce the electricity bill. The last strategy (strategy 3) is based on a fast charging station for city buses. In this strategy the objective is to reduce the contracted grid power, by having the SLB contributing to the charging power of the city bus.

Experimental validation during more than three weeks of operation in each of the scenarios has demonstrated that the SLB degrades more performing in the fast charging station for urban buses (strategy 3), mainly in terms of capacity, which is due to the greater requirements in the operating conditions of the SLB compared to the rest of the scenarios. It is expected that in this type applications, more demanding for the storage system, it will be necessary to oversize the SLB in order to guarantee economic profitability.

In conclusion, the performance of a repurposed battery with modules from EVs has been experimentally validated under three operating scenarios. Consequently, this paper contributes to demonstrate the technical feasibility of SLBs in applications related to residential microgrids and electric mobility.

REFERENCES

[1] International Energy Agency, Global EV Outlook 2021, Paris, 2021.

[2] E. Martinez-Laserna, I. Gandiaga, E. Sarasketa-Zabala, J. Badeda, D.-I. Stroe, M. Swierczynski, A. Goikoetxea, “Battery second life: Hype, hope or reality? A critical review of the state of the art”, Renewable and Sustainable Energy Reviews, Volume 93, 2018, pp. 701-718.

[3] E. Braco, I. San Martin, A. Berrueta, P. Sanchis, A. Ursua, “Experimental Assessment of First- And Second-Life Electric Vehicle Batteries: Performance, Capacity Dispersion, and Agin,” IEEE Transactions on Industry Applications, 57 (4), art. no. 9416769, 2021, pp. 4107-4117.

[4] E. Hossain, D. Murtaugh, J. Mody, H. M. R. Faruque, M. S. Haque Sunny and N. Mohammad, "A Comprehensive Review on Second-Life Batteries: Current State, Manufacturing Considerations, Applications, Impacts, Barriers & Potential Solutions, Business Strategies, and Policies," in IEEE Access, vol. 7, 2019, pp. 73215-73252.

[5] L. Canals Casals, B. A. García, C. Canal, “Second life batteries lifespan: Rest of useful life and environmental analysis”, Journal of Environmental Management, vol. 232, 2019, pp. 354-63.

[6] M. Shahjalal, P. K. Roy, T. Shams, A. Fly, J. I. Chowdhury, Md. R. Ahmed, K. Liu, “A review on second-life of Li-ion batteries: prospects, challenges, and issues”, Energy, vol. 241, 2022, 122881.

[7] J. W. Lee, M. H. S. M. Haram, G. Ramasamy, S. P. Thiagarajah, E. E. Ngu, Y. H. Lee, “Technical feasibility and economics of repurposed electric vehicles batteries for power peak shaving”, Journal of Energy Storage, vol. 40, 2021, 102752.

[8] C. White, B. Thompson, L. G. Swan, “Repurposed electric vehicle battery performance in second-life electricity grid frequency regulation service”, Journal of Energy Storage, vol. 28, 2020, 101278.

[9] E. Braco, I. San Martin, A. Berrueta, P. Sanchis, A. Ursua, “Experimental assessment of cycling ageing of lithium-ion second-life batteries from electric vehicles”, Journal of Energy Storage, 32, 2020, 101695.

[10] H. Rallo, L. Canals Casals, D. De La Torre, R. Reinhardt, C. Marchante, B. Amante, “Lithium-ion battery 2nd life used as a stationary energy storage system: Ageing and economic analysis in two real cases”, Journal of Cleaner Production, vol. 272, 2020, 122584.

[11] Y. Gao, Y. Cai, C. Liu, “Annual operating characteristics analysis of photovoltaic-energy storage microgrid based on retired lithium iron phosphate batteries”, Journal of Energy Storage, vol. 45, 2022, 103769.

[12] J. Lacap, J. W. Park, L. Beslow, “Development and Demonstration of Microgrid System Utilizing Second-Life Electric Vehicle Batteries”, Journal of Energy Storage, vol. 41, 2021, 102837.

[13] S. J. Tong, A. Same, M. A. Kootstra, J. W. Park, “Off-grid photovoltaic vehicle charge using second life lithium batteries: An experimental and numerical investigation”, Applied Energy, vol. 104, 2013, pp. 740-750.

[14] X. Han, Y. Liang, Y. Ai, J. Li, “Economic evaluation of a PV combined energy storage charging station based on cost estimation of second-use batteries”, Energy, vol. 165, Part A, 2018, pp. 326-339.

[15] R. Ghotge, A. Wijk, Z. Lukszo, “Off-grid solar charging of electric vehicles at long-term parking locations”, Energy, vol. 227, 2021, 120356.

[16] C. Galilea, J. Pascual, A. Berrueta, A. Ursua and L. Marroyo, "Economic analysis of residential PV self-consumption systems with Li-ion batteries under different billing scenarios”, 2019 IEEE International Conference on Environment and Electrical Engineering and 2019 IEEE Industrial and Commercial Power Systems Europe (EEEIC / I&CPS Europe), 2019, pp. 1-6.

[17] I. Ojer I., A. Berrueta, J. Pascual, P. Sanchis, A. Ursua. “Development of energy management strategies for the sizing of a fast charging station for electric buses”, 2020 IEEE International Conference on Environment and Electrical Engineering and 2020 IEEE Industrial, 2020.

[18] I. San Martín, A. Berrueta, P. Sanchis, A. Ursúa, “Methodology for sizing stand-alone hybrid systems: A case study of a traffic control system”, Energy, vol. 153, 2018, pp. 870-81.